A Case Study of a Natural Gas Pipeline Failure Due to CP-Related Hydrogen-Assisted Cracking

Pablo Cazenave, Ming Gao, Katina Jimenez and Ravi Krishnamurthy
Blade Energy Partners

Pipeline Pigging and Integrity Management Conference

February 12-16, 2024

CLARION
TECHNICAL CONFERENCES

Organized by
Clarion Technical Conferences

https://doi.org/10.52202/072781-0065

https://doi.org/10.52202/072781-0065

Abstract

The possibility of hydrogen-induced cracking and hydrogen-assisted cracking as interactive threats is increasingly becoming a safety concern to pipelines. While few cases exist of fully documented onshore transmission pipeline failures due to CP-related hydrogen-assisted cracking, the possibility of hydrogen-assisted failures needs further investigation, particularly hydrogen interacting with stress corrosion cracking in very negative cathodic potentials.

This paper presents a case study, of a 22-inch onshore natural gas transmission pipeline that experienced in-service leaks and a rupture associated with axially and circumferentially oriented crack colonies. The colonies were initially thought to be traditional stress corrosion cracking. In-depth metallographic examination revealed cracking fracture paths consistent with hydrogen-assisted cracking. Further investigation of potential sources of hydrogen concluded that the source is the impressed-current cathodic protection system, operated for decades at near the P/S potentials of −1200 mV CSE.

An approach to mitigating the threat of hydrogen-induced cracking in onshore pipelines is also outlined.

https://doi.org/10.52202/072781-0065

Background

An in-service pipeline rupture occurred on January 18th, 2018, involving a 22-inch onshore natural gas transmission pipeline in Argentina. The rupture occurred approximately 150 km (93 miles) downstream of the closest upstream compression station.
Operated by Transportadora de Gas del Norte (TGN), this pipeline, constructed in 1960 with API 5L X52 steel, has a nominal diameter of 22 inches (558.8 mm) and a nominal wall thickness of 0.250 inches (6.35 mm). Constructed with pipe fabricated by A.O. Smith (USA), the initial 118 Km (74 mi) features a longitudinal Electric Flash Welded (EFW) seam weld, while the subsequent 34 Km (21 mi) consists of seamless pipe. Both are coated with asphalt. The design pressure (DP) and Maximum Allowable Operating Pressure (MAOP) line up at 59.8 Kg/cm2 (850 psi, 72% of the Specified Minimum Yield Strength - SMYS).

TGN meticulously investigated the incident, recovering two pipe fragments on-site. The rupture's origin was traced back to two deep external axial cracks at orientation 3:00. Magnetic particle inspection (MPI) was conducted on the external surface and exposed colonies of axial cracks adjoining the fracture edges.

During the root cause analysis in March 2018, TGN conducted excavations commencing 190 Km (118 miles) downstream of the compression station and 42 km (26 miles) downstream of the rupture. These excavations aimed to investigate indications identified by a Hard Spot In-Line Inspection (ILI). The excavations unveiled predominantly circumferential crack colonies, with several through-wall cracks leading to leaks.

TGN meticulously documented the crack locations, undertaking the necessary repairs and replacements. Additionally, hydrostatic pressure tests were conducted on removed pipes to measure the actual failure pressure associated with the most severe circumferential cracks.

Investigation

TGN and Blade meticulously documented the areas exhibiting cracks during both in-ditch and on-site investigations to confirm and document the presence of cracks and crack colonies. The reconstruction process involved assembling the original pipe (cylinder) based on the recovered parts, which included detailing the rupture origin and the paths of crack propagation. Magnetic Particle Inspection (MPI)-identified crack colonies, along with the relative positioning of seam and girth welds, were mapped. The reconstruction highlighted numerous crack colonies both up- and down-stream of the rupture origin, and in varied orientations.

Fourteen (14) panels were excised from the ruptured pipe sections and dispatched to Houston for root cause analysis (RCA). Among these panels, seven (7) exhibited circumferential cracks, some of

https://doi.org/10.52202/072781-0065

which had leaked during the excavations. Additionally, two (2) panels from undeformed pipes without defects were reserved for material testing of the base material and coating testing.

The comprehensive protocol adopted for the assessment of the coating condition involved the visual examination of the coating and the steel substrate, the identification of the coating material, the measurement of the coating thickness, the measurement of the porosity across the coating thickness and on the surface in contact with the steel substrate, the measurement of the water absorption of the coating and the analysis of the nature of the deposits and whitish crystals found at the coating-steel interface.

The in-lab coating evaluation identified it as asphalt enamel with fiberglass reinforcement. The observed characteristics indicate that the coating is brittle, displaying poor adhesion to the pipe surface. Despite being hygroscopic, the coating absorbs minimal water. It exhibits signs of aging, yet it is highly probable that the cathodic current can efficiently flow through it to protect the underlying steel. Further analysis of whitish deposits and crystals identified them as calcite (CaCO3).

The in-ditch photographic documentation revealed similar coating characteristics across the investigated locations: it is brittle and poorly adhered, there was no significant corrosion, suggesting that it has provided a degree of protection against corrosion, and the interface between the coating and the metallic pipe surface contains contaminants such as soil, whitish, and reddish deposits, see Figure 1.

Figure 1: Coating condition and whitish deposits found in excavations

The combined findings from the coating evaluation and in-ditch photographic documentation show that the coating has aged and probably does not cause the shielding of the cathodic protection. The absence of significant corrosion and the whitish residues indicate that the pipe has been cathodically protected against corrosion.

https://doi.org/10.52202/072781-0065

The soil resistivity data collected at a depth of 1.50 meters (5 feet) was also reviewed, showing that the soil resistivity is low in the areas where cracks were identified, varying between 600 and 1800 Ohm-cm.

The soil is identified as clayish or silty with good drainage capabilities. In clayier areas, saturation with water can occur during the rainy season. As the area is extensively used for agriculture, there is a probability that the soil is contaminated with fertilizers and organic or chemical pesticides. Based on the resistivity, the soil adjacent to the sites of verification excavations is classified as corrosive to moderately corrosive[1].

In summary, although the soil is classified as corrosive, its type allows for less resistance to the cathodic protection (CP) current. This characteristic enables the CP to flow and distribute easily through the soil, facilitating adequate protection of the pipeline.

The cathodic protection system for this pipeline section operates under the criterion of 100 mV polarization[2]. The cathodic protection (CP) data was reviewed, including the records detailing the operating performance of rectifiers over the past decade, the depolarized Potential Data for 2009 and 2015, three Pipe-to-Soil (P/S) potential surveys conducted in 2009, 2014, and 2017, the last ten years of ON P/S potentials from April 2008 to February 2018, and the IR-free potentials calculated for 2016 and 2017.

The monthly records of DC outputs and ON-OFF potentials measured at the rectifiers over the last ten years reveal that the equipment has been consistently operational. While there were occasional short periods of non-operation, the overall continuity of the equipment indicates a sustained effort to uphold cathodic protection for the pipeline section.

Figure 2 shows the ON, OFF (IR-free) surveys and depolarized potentials in the section around the rupture carried out in 2009 and 2015. These data are aligned and aggregated with the soil resistivity, elevation, and depth of external corrosion surveyed by the 2013 ILI (MFL). It is observed that the depolarized potentials vary between -550 and -350 mV CSE and that the 2015 depolarized potential records show a change in the most positive direction in the rupture area.

https://doi.org/10.52202/072781-0065

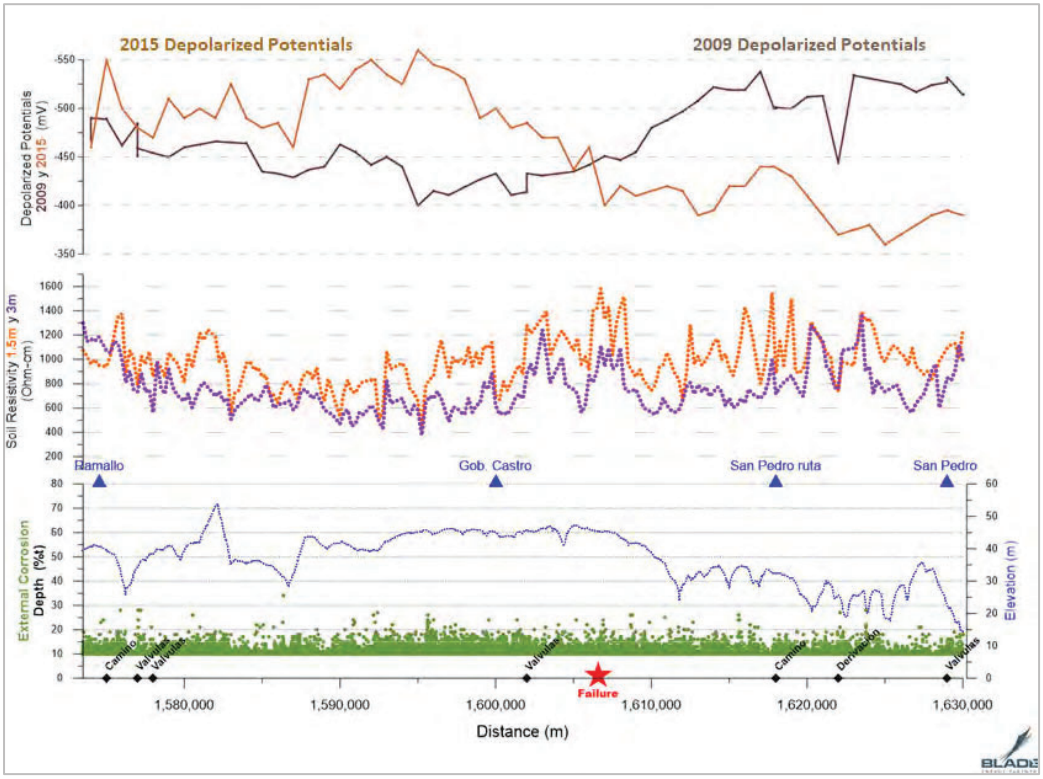

Figure 2: CP potentials in the area of the rupture

Regarding the cathodic P/S potential levels of the section, they comply with current NACE[2] and ISO[3] practices and recommendations. The OFF pipe-to-soil potentials have been kept very close to the recommended limit of -1200 mV CSE, and the polarization of this pipe section tends to increase over time (see **Figure 3**). In the zone adjacent to the rupture, when comparing OFF and depolarized potentials, the level of polarization in the area adjacent to the rupture increased.

https://doi.org/10.52202/072781-0065

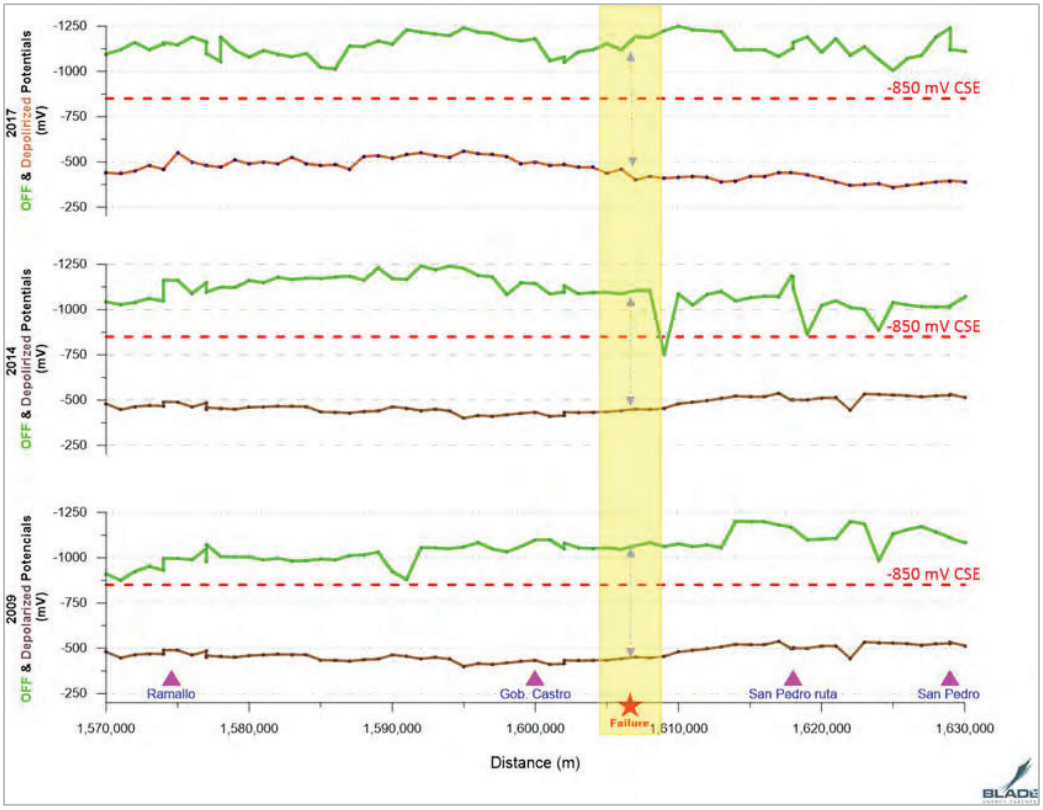

Figure 3: Historic OFF and depolarized potentials near the rupture area

Cathodic protection reactions cause atomic hydrogen formation on the metal's surface. Hydrogen generation is an electrochemical reaction that occurs on the surface of all cathodically protected pipelines, and the speed of that reaction increases with the applied CP current. Within the cathodic polarization range of -850 to -1200 mV CSE, the hydrogen generation increases towards the more negative potential limit. The review of the CP data concludes that, at the test points in the vicinity of the rupture site, the pipe has been cathodically polarized at potentials very close to the NACE-recommended limit of -1200 mV CSE.

The review of pressure records involved the application of the Cumulative Damage Approach, utilizing the Rainflow and Miner's Rule methods. This analysis aimed to calculate the equivalent number of cycles per year for the rupture location based on hourly pressure records. The same calculations were repeated for various locations within the gas pipeline system to facilitate comparison.

The findings indicate that pressure cycling is generally low across all locations, specifically at 13.3 cycles per year with a pressure range of 300 psi. This low cycling frequency is in line with the operational characteristics of gas transmission pipelines operating near total capacity.

The metallurgical evaluation of the pipeline rupture included the visual and stereoscopic macro examination of the fracture surfaces, the micro fractographic examination with Scanning Electron

https://doi.org/10.52202/072781-0065

Microscopic (SEM) and Energy Dispersive Spectroscopic (EDS) examination of fracture surfaces at a microscopic level, the analysis of the material's microstructure and crack paths in relation to the microstructure of the pipe body steel, and comprehensive material testing involving the determination of chemical composition of the pipe body steel, tensile testing, Charpy V-notched impact testing, and fracture mechanics testing for J-R curve measurements.

The rupture origin was confirmed by examining the fracture surface, guided by the direction of chevron marks. Chevron marks were identified on both sides of the origin, pointing towards the rupture origin and opposite to the crack propagation direction.

The rupture origin crack has a total length of 221mm, with a peak depth of 5.78mm (91% wall thickness). The rupture origin comprises multiple cracks that coalesced during the rupture event, exhibiting steps between adjacent-coalesced cracks. Importantly, these initiating cracks are located in the pipe body and are not associated with welds or corrosion.

In addition, in the areas where the leaks occurred, none of the cracks are linked to external corrosion. Instead, the panels exhibit a complex pattern of multiple circumferential and spiderweb cracks (see Figure 4), some penetrating through the wall and causing leaks.

https://doi.org/10.52202/072781-0065

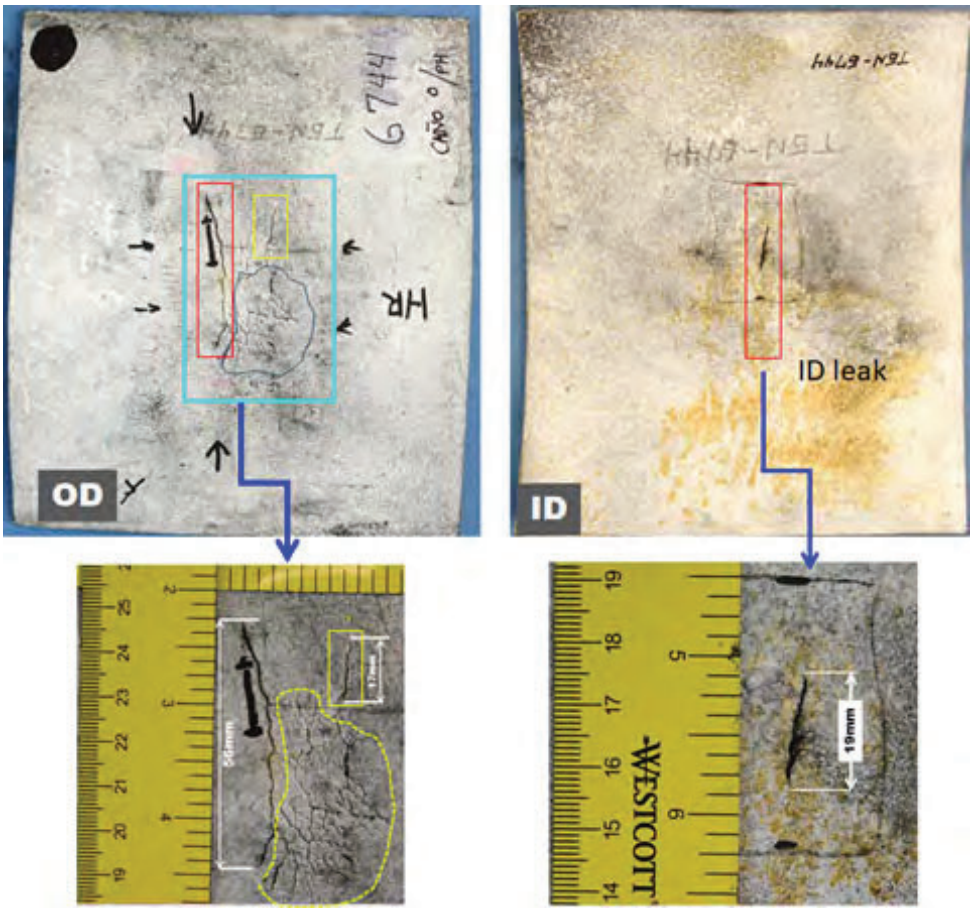

Figure 4: Example of circumferential and spiderweb cracking in the leaking areas

Cracks and crack fields observed in the base-metal (pipe body) of transmission pipelines can generally be classified into four types based on their orientation and appearance on a macroscopic scale: longitudinal (axial), circumferential (transverse), inclined (in-between), and spiderweb cracks. These classifications help understand the cracks' potential implications for pipeline integrity and are primarily related to the failure pressure.

Conversely, the classification of crack types based on their macroscopic characteristics does not inherently provide insights into the underlying cracking mechanism, as there is no consistent correlation between the macroscopic crack morphology and the micro-level cracking mechanisms. For instance, crack fields resulting from fatigue in dents in liquid transmission pipelines were historically identified[4] as stress corrosion cracking (SCC). Since it is essential to understand the cracking mechanism for developing an integrity plan for crack management, the overall goal of the metallurgical investigation is to identify the mechanism for the occurring cracks.

In pipelines transporting natural gas, the cracking mechanism for time-dependent failure is one of the following: near-neutral pH SCC (NNpHSCC), high pH SCC (HpHSCC), hydrogen environment assisted cracking (HEAC), environmentally assisted fatigue crack growth, or others such as mechanical delayed rupture by plasticity-induced cracking[5,6,7].

https://doi.org/10.52202/072781-0065

The samples containing the rupture's origin were cleaned to remove the superficial corrosion deposits and scales, and the fracture surface of the origin near the crack tip was then examined. Figure 5 shows the fracture surface morphology of the origin near the crack tip at various magnifications. At higher magnifications, as shown in Figure 5c and d, the appearance of the fracture surface is featured with cleavage facets, typical of cracking produced by hydrogen embrittlement with high hydrogen fugacity.

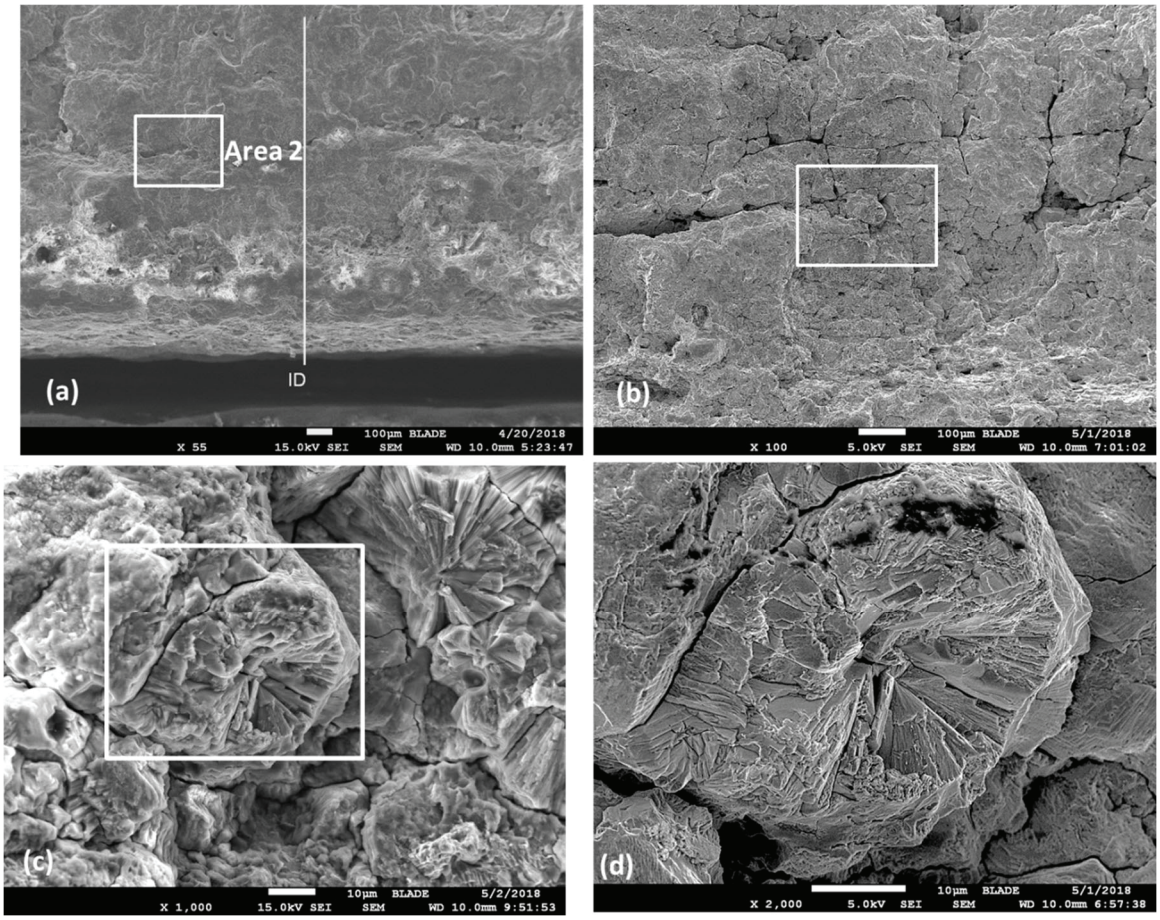

Figure 5: Fracture surface morphology near the crack tip at various magnifications

This type of cleavage facets cannot be produced by corrosion; they are also inconsistent with those produced by high pH SCC, near-neutral pH SCC, or fatigue. It is noted that these cleavage facets were generally observed near and along the crack-tip region where the fracture surface was most recently formed with little corrosion under high cathodic potential conditions. Figure 6 shows the cleavage facets observed along the crack region.

https://doi.org/10.52202/072781-0065

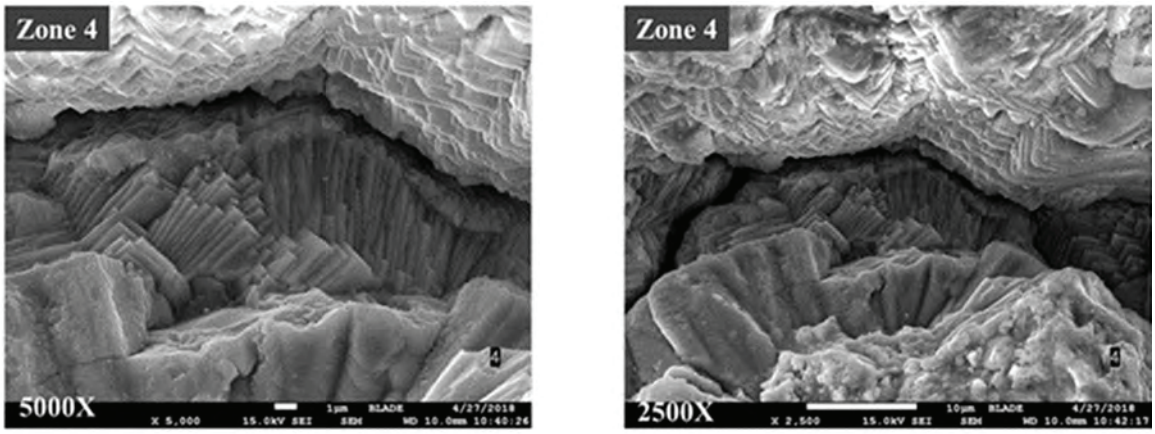

Figure 6: Cleavage facets along the crack tip region – 2500X and 5000X

Further EDS analysis of the cleavage facets shows the facets free of oxide scale, as demonstrated by a high peak of iron and very low oxygen peak, and with some minor Mn and Si peaks that are part of the composition of X52. Similar EDS results are obtained from other cleavage facets, commonly showing higher iron (Fe) and nil oxygen (O) peaks. The findings confirm that the newly formed fracture surfaces have minor corrosion, as shown in Figure 7.

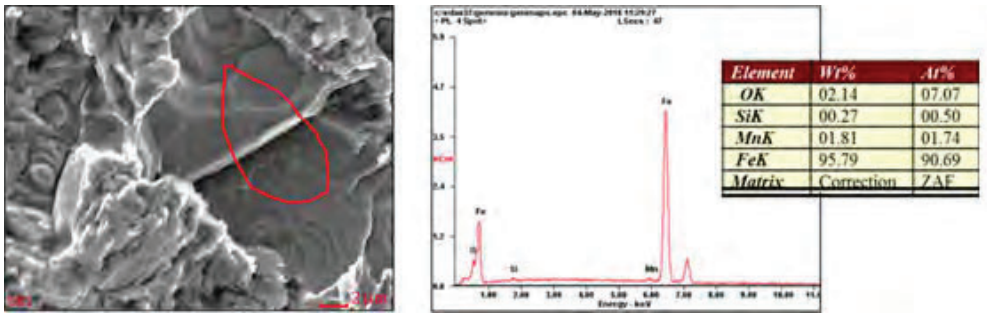

Figure 7: EDS spectrums

Similar Cleavage Facets were observed in a refined products pipeline system studied[8] by the authors in North America. Figure 8 shows the mirrored cleavage facets on the mated surfaces of circumferential cracks in the referred pipeline. As corrosion cannot produce mirrored cleavage facets because it is an independent event on each side of the fracture surface, these cleavage facets can only be made by hydrogen cracking[9,10,11].

They are also inconsistent with those produced by high pH or near-neutral pH SCC or fatigue. The morphologies observed in TGN's samples are consistent with the ones observed in this refined products pipeline, which are also related to very negative CP potentials that produce high fugacity hydrogen at the crack tip.

Hydrogen-induced cracks including cleavage are commonly observed to initiate at micro-defects such as inclusions, micro-cracks, and cross-slip bands. It is a widely recognized phenomenon that the presence of hydrogen exacerbates the susceptibility of these micro-defects to crack initiation.

https://doi.org/10.52202/072781-0065

However, it's crucial to note that while evidence highlights the significance of inclusions, it's not always the case that inclusions are observed at the center of hydrogen-induced cleavage.

Other types of micro-defects can also contribute to the initiation of hydrogen cracking. Micro-cracks and cross-slip bands, for example, may play a role in facilitating the initiation of hydrogen-induced cleavage. This underscores the complex nature of hydrogen-induced cracking mechanisms and the need for a comprehensive understanding of various micro-level factors that can contribute to crack initiation. Identifying and addressing these micro-defects is essential for developing effective strategies to mitigate hydrogen-induced cracking and ensure the integrity of the material.

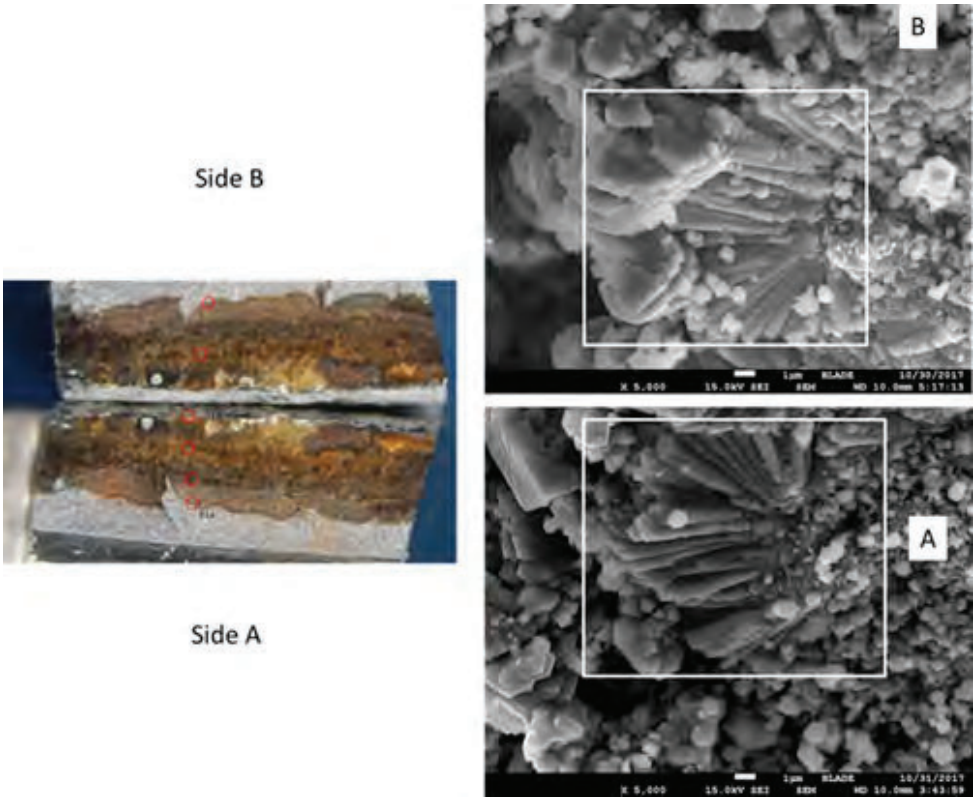

Figure 8: Mirrored cleavage facets of mated surfaces - Hydrogen-induced cracking observed in a pipeline in the USA

Cracks in the colonies near the rupture origin were also broken open and examined in SEM for fractography. Figure 9 below shows the facture morphology at the tip. The view at higher magnifications of the areas outlined with blue boxes reveals the presence of microcrystals.

The EDS spectrum of the microcrystals in Figure 10, in a location close to the crack-tip, shows a large iron (Fe) peak and a small oxygen (O) peak, suggesting the microcrystals are ferrite without oxide scales. This type of microcrystal of ferrite was also observed in the previously mentioned study of cracking in the pipeline in the US. The EDS analysis performed during that investigation showed that these micro-crystals were pure ferrite crystals, consistent with the present study.

https://doi.org/10.52202/072781-0065

It is also noted that the sizes of the microcrystals are in order of magnitude of several microns, which seem to be consistent with the dimensions of sub-grains of ferrite as observed in low-carbon steel. Therefore, these microcrystals found in the present and previous studies might be formed by hydrogen cracking of the sub-grains of ferrite. However, further fundamental research is needed to confirm and understand the observed phenomenon.

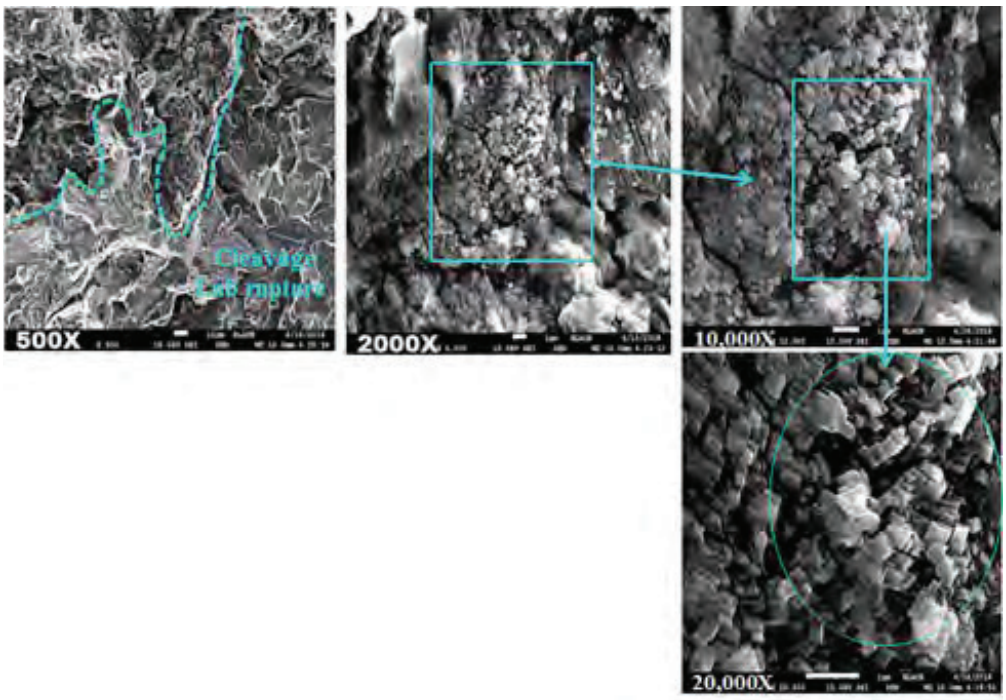

Figure 9: Morphology micro-crystals on the fracture surfaces at 500X, 2000X, 10000X and 20000X

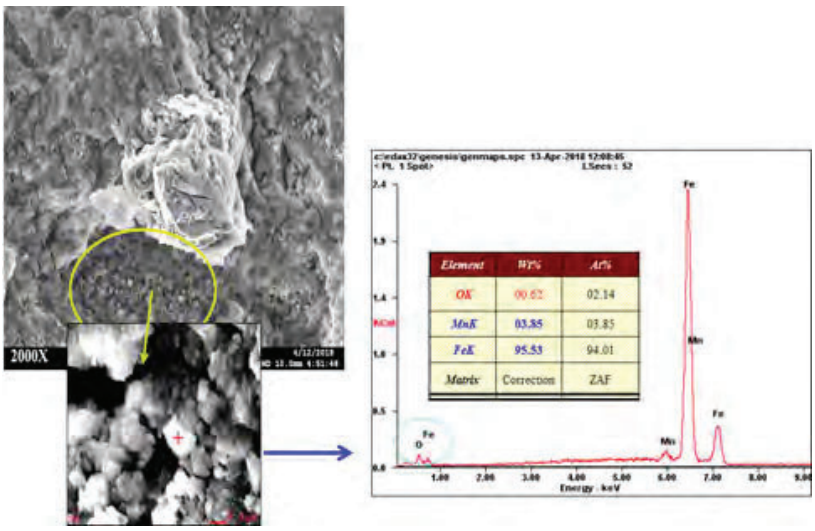

Figure 10: SEM/EDS analyses for a location close to crack-tip

https://doi.org/10.52202/072781-0065

In addition, microcracks associated with breaking inclusion/ base metal by hydrogen were also observed. It is commonly known[12,13,14] that the interface between inclusion and steel matrix in the steels is the favorable site for cracking because of their differences in elastic modulus and mismatch in crystal structure. Moreover, the interface also acts as a trapping site for hydrogen.

The accumulation of hydrogen molecules in those trapping sites that resulted in the interface cracking is well documented in the literature[12,13,14], and Figure 11 and Figure 12 show the respective optical microscope examination of polished and etched cross-sections of a sample close to the ruptured area, showing microcracks that are associated to manganese sulfide (MnS) inclusions.

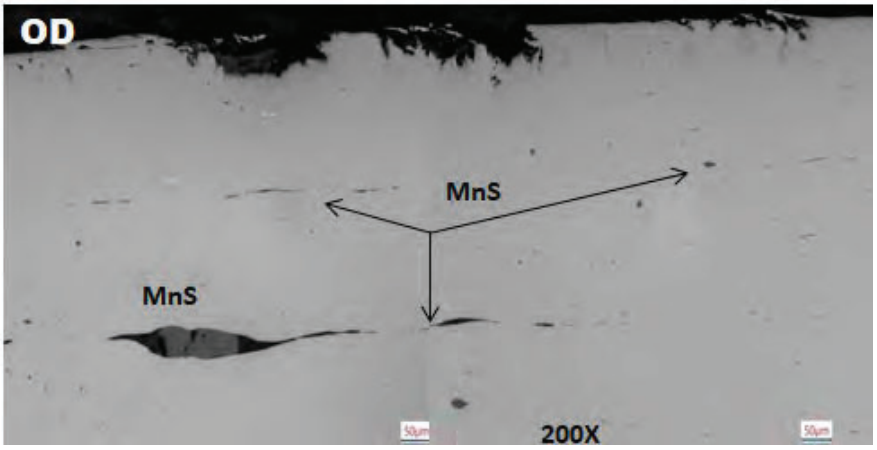

Figure 11: Microcracks associated with inclusions near the ruptured crack

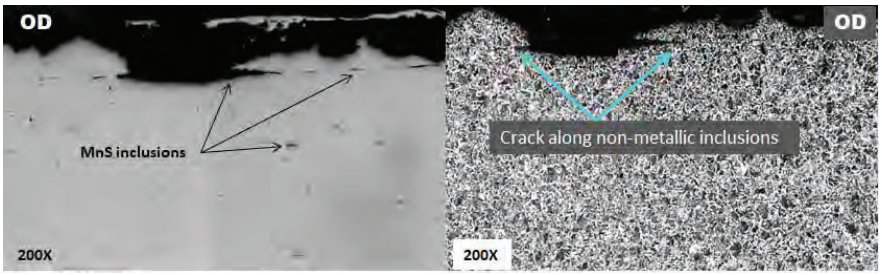

Figure 12: Etched longitudinal cross-section of base metal

Furthermore, Figure 13 and Figure 14 show details of the evaluation with an optical microscope of a polished cross-section adjacent to the main crack, where numerous microcracks associated with the inclusions of MnS are observed.

The figures show optical micrographs of the polished cross-section of axial cracks, where branching features are visible along the main crack path. Multiple crack ramifications and micro-cracks associated with the close inclusions are observed at increasing magnification, consistent with the hydrogen-induced cracking mechanism.

https://doi.org/10.52202/072781-0065

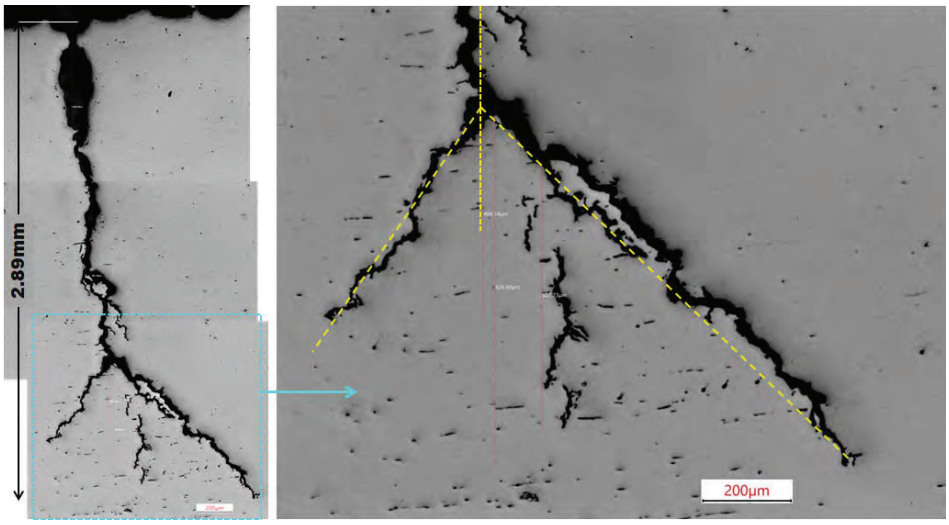

Figure 13: High concentration of microcracks in inclusions near the ruptured crack

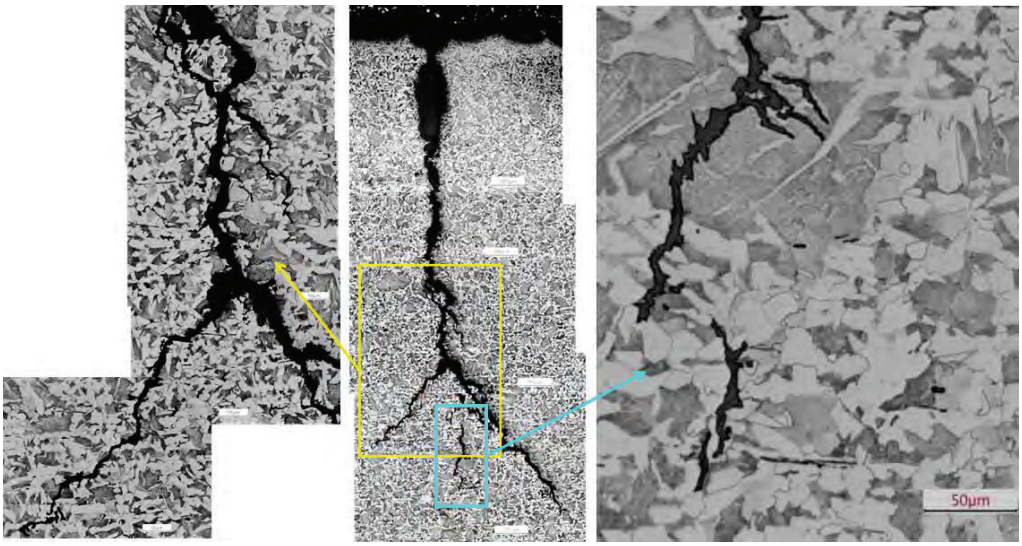

Figure 14: Details of the cracks (etched)

The microstructure of the pipe body metal was also analyzed. Metallographic analyses were performed in transverse and longitudinal cross-sections near and far from the crack colonies. All the locations evaluated showed a Widmanstädter microstructure (acicular ferrite with pearlite or pearlite colonies distributed in an acicular ferrite matrix), which differs significantly from the expected microstructure of a typical linepipe X52 steel. On the other hand, and with the same level of metallographic analysis performed, the hydrogen cracks in the liquid pipeline evaluated (see Figure 8) were associated with a non-acicular ferrite and pearlite microstructure. Consequently, more work is needed to understand the relative susceptibility of pipeline steels to this phenomenon.

The same specimens were tested for hardness. Hardness near cracked areas is similar to hardness away from cracked areas and well below the hard spot threshold. Consequently, the hydrogen cracking found in this study is not associated with hard spots.

https://doi.org/10.52202/072781-0065

Based on the study's findings, Transportadora de Gas del Norte (TGN) has revamped its Integrity Management Program to address the new threat posed by hydrogen cracking in its pipeline system. The updated program incorporates both preventive and corrective measures, including:

1. Training of Integrity Staff: Implementation of training programs for the Integrity staff to enhance their understanding of hydrogen cracking phenomena.
2. Immediate Reduction of Hydrogen Generation: Prompt adjustment of the cathodic protection system to immediately reduce hydrogen generation while maintaining the pipeline within protection limits.
3. Expansion of the Direct Assessment Plan: Expansion of the Direct Assessment Plan to detect and address additional cracks similar to those that led to the failure.
4. Implementation of Hydrostatic Testing: Hydrostatic testing in the ruptured section is introduced to assess and ensure the pipeline's structural integrity.
5. Installation of Semiautomatic CP Equipment: Installation of semiautomatic cathodic protection (CP) equipment with multiple outputs to achieve a more efficient distribution of CP current. This aims to minimize high hydrogen generation by directing current to sections with lower requirements.
6. Development of Metallographic Database: Establishment of a comprehensive metallographic database for the entire pipeline system. This involves incorporating steel samples obtained in excavations and subjecting them to subsequent laboratory analysis. This database serves as a valuable resource for ongoing pipeline integrity assessments.
7. Extension of Corrosion and Crack Growth Assessments: Extending corrosion and crack growth assessments to address potential threats comprehensively.
8. Inclusion in Risk Assessment: Incorporating the hydrogen cracking threat into the risk assessment software and relevant database for a holistic evaluation.
9. Additional Line Inspections: Conducting additional runs of Line Inspection technologies, including Electromagnetic Acoustic Transducer (EMAT) for crack detection and Determination of Pipe Grade.

The Failure Analysis determined that the asphalt coating at the rupture site was highly deteriorated, exposing the metal surface to the soil electrolyte and facilitating the hydrogen-generating cathodic reaction. Consequently, a comprehensive coating evaluation via EMAT In-Line Inspection (ILI) and recoating of parts of the pipeline section was scheduled, with the initial phase implemented in 2019. Moreover, adjustments to the current distribution of cathodic protection were implemented to reduce polarization levels. These proactive measures underscore TGN's commitment to ensuring the safety and reliability of its pipeline system.

https://doi.org/10.52202/072781-0065

Conclusions

The investigation concludes that the in-service rupture of a 22-inch onshore natural gas transmission pipeline on January 18th, 2018, resulted from environmentally assisted hydrogen cracking. The following key observations support this determination:

- The cracks evaluated are not high pH stress corrosion cracking (HpHSCC)
    - HpHSCC is characterized by intergranular cracking.
- They are not NNpHSCC
    - For NNpHSCC, the fracture mode is invariably quasi-cleavage[15,16] while for HAC, the fracture mode is cleavage or cleavage mixed with quasi-cleavage in low-strength carbon steels. The fracture modes can only be fully characterized with detailed fractographic SEM work.
    - For NNpHSCC, the hydrogen source is the cathodic reaction at the crack tip and the OD steel surface. In a near-neutral pH environment, the metal in the crack tip region is dissolved, assisted by stress concentration associated with galvanic corrosion cells. For HAC in pipelines, the hydrogen source is also associated with cathodic reactions, but those that can generate more hydrogen than the one required for NNpHSCC[17], like the reactions that occur in SRB MIC and in the Cathodic Protection by ICCP. In other words, cleavage cracking requires a higher amount and fugacity of hydrogen than quasi-cleavage.
- They are not Fatigue/Corrosion Fatigue
    - There is no evidence of fatigue or corrosion fatigue, as evidenced by the absence of corresponding patterns in pressure cycling or fatigue striations on the fracture surface.
- They are not associated with Microbiological Corrosion (MIC)
    - Typical microbiological corrosion, such as that caused by sulfate-reducing bacteria (SRB), is ruled out. The transported product is not sour, and there are no internal cracks (ID) resulting from MIC.
- They are not associated with hard spots
    - No hard spots were found in or around the cracked areas.

The review of the historical CP readings suggests that the only possible source of the high amount of hydrogen is associated with the ICCP systems, operated near the most negative range of pipe-to-soil potentials over long periods of past operation.

Therefore, the plausible root cause for the observed hydrogen cracking appears to be the combination of a defective coating, the ICCP system operated for extended periods (decades) at a pipe-to-soil potential close to −1200mV CSE, and the presence of a susceptible material.

https://doi.org/10.52202/072781-0065

Discussion of Effects of CP-related Hydrogen Generation in Other Types of Cracking

Argentina has a 39,000 km long high-pressure pipeline system transporting natural gas from production fields to local and exporting markets. This system's primary natural gas pipelines are 24, 30, and 36 inches in diameter, more than 60 years old, and coated with asphalt enamels that have severely degraded over time.

The pipelines were constructed in the late 50s and 60s and maintained by the state-owned Gas del Estado company until 1992, when the system was privatized. Since 1992, two private companies have operated the high-pressure pipeline system, TGS (Transportadora de Gas del Sur) and TGN (Transportadora de Gas del Norte).

The natural gas pipeline system had several in-service and during-hydrotest failures at crack colonies[18] and has a long history of operating the CP systems near the most negative side of the potentials. Most of these failures were attributed to High pH SCC (HpHSCC), and TGN and TGS worked to develop a susceptibility model[19] for HpHSCC. At a time when crack detection ILI systems capable of running in gas were in early development, the model was applied with success to manage the SCC threat.

Within other soil and terrain considerations, the model showed that most failures occurred close to compression stations and in areas where the asphalt coating was in poor condition with no external corrosion, conditions consistent with HpHSCC. It also showed that most failures occurred close to cathodic protection rectifiers (less than 3 km) in areas with high CP current output, more consistent with high hydrogen generation than with HpHSCC.

In late 2010 and early 2011, there were two ruptures in areas where the SCC model deemed them unlikely. A review of the root cause analyses of these two failures performed by the authors in late 2012 showed that the crack colonies were inconsistent with HpHSCC. One of the failures was caused by a manufacturing defect, a hard spot with cracks on a low-toughness Electric Resistance Welding (ERW) seam weld. The other one was related to transgranular cracking found in a hard spot, and probably related to hydrogen cracking. The hydrogen-induced cracking could have been most likely associated with extended cathodic over-potential on a susceptible microstructure. However, the CP data and coating conditions were unavailable during this investigation.

A more detailed review of the failure analysis reports showed incomplete characterization of the fracture surfaces. In addition, further revision of the older failure analysis reports (all deemed to be HpHSCC) found the fracture surfaces looked intergranular, with α-ferrite + pearlite microstructures consistent with High pH SCC; however, it also found that the review of the fracture surfaces was neither complete to establish a complete HpHSCC characterization nor sufficient to evaluate the effects of hydrogen in the fracture surfaces.

https://doi.org/10.52202/072781-0065

In light of the recent HAC/HIC findings in these pipelines, this old evidence can be viewed from a different angle:

- HAC/HIC and HpHSCC may alternate as subcritical crack growth mechanisms, depending on the local and seasonal environmental conditions,
- The effects of the hydrogen embrittlement increase the growth rate of the HpHSCC colonies closer to the CP rectifiers.

The lessons learned from these studies are that more detailed fracture surface analyses, in combination with the review of the historic pressure and CP data, and the local soil and coating conditions, are needed to discern the specific influence of hydrogen in the interaction with other forms of environmentally assisted pipeline cracking.

References

[1] H. C. Van Nouhuys. *"Cathodic protection and high resistivity soil"*, Corrosion, Vol.9, Dec, 1953, 448-459

[2] NACE SP0169-2015, Standard Practice 0169. *"Control of External Corrosion on Underground or Submerged Metallic Piping Systems"*. NACE International, 2015

[3] ISO 15589-1. *"Petroleum and natural gas industries - Cathodic protection for pipeline transportation systems - Part 1: On-land pipelines"*.

[4] U. Arumugam, P. Cazenave, M. Gao. *"Study of the Mechanisms for Cracking in Dents and Material Properties in a 24-inch Crude Oil Pipeline"*. PRCI report, project MD-1N.

[5] PHMSA Failure Investigation Report, *"TransCanada/Bison Pipeline Natural Gas Transmission Release near Gillete, WY"*. November 7, 2012.

[6] Blade Energy Partners. "*Root Cause for Bison Pipeline Failure: Factual Evidence from Supplemental Investigation*", May 28, 2011. Report prepared for PHMSA.

[7] Ingham and E. Morland: *"Influence of Time-Dependent Plasticity on Elastic-Plastic Fracture Toughness"*. ASTM STP 803, 1983, pp. I-721-I-746.

[8] S. Tandon, M. Gao, R. Krishnamurthy. *"Study of axial and circumferential cracking in a 12-inch oil pipeline*". Private report to the pipeline operator.

[9] Qian Liu, *"Influence of hydrogen on metallic components for clean energy*". PhD thesis, The University of Queensland, Australia, 2014.

[10] Q. Liu, B. Irwanto, A. Atrens. *"The influence of hydrogen on 3.5NiCrMoV steel studied using the linearly increasing stress test*". Corrosion Science 67 (2013) 193–203.

[11] Q. Liu and A. Atrens. *"A critical review of the influence of hydrogen on the mechanical properties of medium-strength steels*". Corros Rev 2013; 31(3-6): 85–103.

[12] A.S. Tetelman, W.D. Robertson. *"The Mechanism of Hydrogen Embrittlement Observed in Iron-Silicon Single Crystals"*. 1961.

[13] R.A. Oriani, P.H. Josephic. *"Hydrogen-enhanced Load Relaxation in a Deformed Medium-carbon Steel"*. Acta Metallurgica, Vol.27, No.6, 1979, pp.997-1005.

https://doi.org/10.52202/072781-0065

[14] M. Elboujdaini, W. Revie. "*Effect of Non-Metallic Inclusions on Hydrogen Induced Cracking*". In Damage and Fracture Mechanics, Springer Netherlands, 2009, pp.11-18.

[15] N. Sridhar. "*Perspective on 'Transgranular Stress Corrosion Cracking of High-Pressure Pipelines in Contact with Solutions of Near Neutral pH,' R.N. Parkins, W.K. Blanchard Jr., B.S. Delanty, Corrosion 50, 5 (1994), p. 394-408*". NACE, Journal of Corrosion, Corrosion (2020) Volume 76, Issue 9: 799–802.

[16] J.A. Beavers and B. A. Harle. "*Mechanisms of High-pH and Near-Neutral-pH SCC of Underground Pipelines*". Paper IPC1996-1860. Proceedings of the ASME 1996 International Pipeline Conference. June 9-14 1996, Calgary, Alberta, Canada.

[17] B. Fang, R. Eadie and M. Elboujdaini. "*Crack Initiation: Stress-Corrosion Crack in X-52 Pipeline Steel in Near-Neutral pH Solution*". Paper IPC2010-31222. September 27-October 1, 2010, Calgary, Alberta, Canada.

[18] Silva, F., Carzoglio, E.J., and Hryciuk, P. "*Rehabilitación al servicio de un gasoducto que ha sufrido una ruptura en servicio por SCC. (Restoration to service of a pipeline that has suffered a rupture due to SCC)*". Rio Pipeline 2003, IBP501_03, 2003.

[19] E. Carzoglio, D. Falabella and M. Corsico. "*Progress in the development of the model for finding High pH SCC in Argentina*". Rio Pipeline 2011, Rio de Janeiro, Brazil. 2011.

https://doi.org/10.52202/072781-0065

https://doi.org/10.52202/072781-0065